Phytoplankton Discrimination Method with Wavelet Descriptor Based Shape Feature Extracted from Microscopic Images

Kohei Arai [1]

[1] Graduate School of Science and Engineering, Saga University, Japan

arai@is.saga-u.ac.jp

Abstract. Image retrieval method based on Euclidian distance between normalized features with their mean and variance in feature space is proposed. Effectiveness of the normalization is evaluated together with a validation of the proposed image retrieval method. The proposed method is applied for discrimination and identifying dangerous red tide species based on wavelet utilized classification methods together with texture and color features. Through experiments, it is found that classification performance with the proposed wavelet derived shape information extracted from the microscopic view of the phytoplankton is effective for identifying dangerous red tide species among the other red tide species rather than the other conventional texture, color information. Moreover, it is also found that the proposed normalization of features is effective to improve identification performance. A visualization method for representation of 3D object shape complexity based on the proposed wavelet descriptor is proposed together with its application to image retrievals. Image retrieval method using wavelet descriptor of shape information together with hue and texture information of objects extracted with dyadic wavelet transformation is proposed. Although there are conventional methods for image retrievals with hue and texture information, image retrieval performance (hit ratio) is not so high.

Therefore, the proposed method uses shape information derived from objects extracted from original images in addition to the hue and texture information. In order extract object, dyadic wavelet transformation is used to find good focusing image area extraction as objects. Experimental results with several kinds of phytoplankton show some improvement of hit ratio as well as Euclidian distance among images.

Keywords: wavelet descriptor; red tide; phytoplankton identification, Image retrieval, Dyadic wavelet, Hue information, Texture information, Wavelet descriptor

1 Introduction

The conventional image retrieval methods use the color information such as HSV 1 : Hue, Saturation and Value (Intensity), RGB: Red, Green, and Blue, etc. as the spectral information. Meanwhile texture information is also used in conventional image retrieval methods as the spatial information. On the other hand, Bachattarian [1], Euclidian2, Mahalanobis3 distance measures [2] are well known as the similarity or distance measure. Not only hierarchical4 and nonhierarchical clustering 5 as well as Bayesian rule of classification6 and Maximum Likelihood classification7, but also Vector quantization8, Support vector machine9, etc. are proposed and used for image retrievals. Relational information such as the relations among image portions or segments, semantic information, knowledge based information, relational similarity to classify semantic relations [3] etc. are tried to use in image retrievals. Spatial and spectral information derived from the images in concern is applicable image retrievals. There are some moment based spatial information extraction methods [4], [5], texture feature based spatial information extraction methods [6] and spectral information based image retrieval methods [7], [8], [9]. Furthermore, some attempts are made for image retrievals with wavelet descriptor as a spatial information extraction [9], [10]. In general, these conventional methods have not so good

performance in terms of retrieval success rate. Image retrieval method based on texture, hue and shape features is proposed [11]. In the proposed method, texture feature is extracted based on discrete wavelet transformation while shape feature is extracted by the proposed wavelet descriptor which allows extraction and representation of contour [12]. Contour of the object extracted from the original image can be expressed with wavelet based descriptor. The image retrieval method which is based on the hue information and texture as well as the wavelet described shape information of extracted objects is proposed previously to improve image retrieval success rate. Image retrieval performance is not good enough in particular for resemble red tide species. The method proposed here is normalization of features in concern with their mean and variance. Through the normalization, all the features used should have almost same influence for discrimination between the current specie and the referenced specie results in improvement of identification performance. The following section describes the proposed image retrieval method followed by some experiments for reproducibility of the proposed wavelet descriptor in comparison to the conventional Fourier descriptor with several simple symmetrical and asymmetrical shapes. Then it is validated with the image database of phytoplankton [13].

There are the following core problems in the image retrieval, (1) Extraction of Visual Signature, (2) Image Similarity Using Visual Signature, (3) Clustering and Classification, (4) Relevance Feedback-Based Search Paradigms, (5) Multimodal Fusion and Retrieval (Prasad et al. 1987 [14], Datta et al. 2008 [15]). Firstly, visual signature, or, object feature has to be extracted. Then image retrieval is made based on image similarity, or, distance between object image features using extracted visual signature. Clustering and classification, in particular, is important to measure the similarity and or distance between extracted visual signatures. Relevance feedback-base search is a new paradigm in image retrievals together with multimodal fusion and retrievals.

Image retrieval success rate (search hit ratio) is not good enough due to a poor visual signature or image feature followed by a poor similarity measure as well as clustering and classification performance. There is some information which can be extracted from images. That is (1) Halftone, color, and spectral information, (2) Spatial information including shape, size, texture, etc., and (3) Relational information such as relation between objects and the other objects included in images. The conventional image retrieval methods use the color information such as HSV : Hue, Saturation and Value (Intensity), RGB: Red, Green, and Blue, etc. as the spectral information. Meanwhile texture information is also used in conventional image retrieval methods as the spatial information. On the other hand, Bachattarian (Duda et al., 2001 [16]), Euclidian , Mahalanobis distance measures (Arai, 1996 [17]) are well known as the similarity or distance measure. Not only hierarchical and non-hierarchical clustering as well as Bayesian rule of classification and Maximum Likelihood classification , but also Vector quantization , Support vector machine , etc. are proposed and used for image retrievals. Relational information such as the relations among image portions or segments, semantic information, knowledge based information, relational similarity to classify semantic relations (Séaghdha, et al., 2009 [18]) etc. are tried to use in image retrievals. Spatial and spectral information derived from the images in concern is applicable image retrievals. There are some moment based spatial information extraction methods (The et al., 1988 [19], Taubin et al., 1991 [20]), texture feature based spatial information extraction methods (Niblack et al., 1993 [21]) and spectral information based image retrieval methods (Zahn et al., 1972 [22], Huang 1998 [23], Yang, 1998 [24]). Furthermore, some attempts are made for image retrievals with wavelet descriptor as a spatial information extraction (Yang 1998 [25], Tieng 1997 [26]). In general, these conventional methods have not so good performance in terms of retrieval success rate.

All the spectral and spatial information are used in image retrieval except shape information. There are some trials to use shape information extracted

from image using Fourier descriptor and the others. There are some definitions for Fourier descriptors. Zahn and Roskies proposed Z type descriptor (Zahn and Roskies. 1972 [27]) while Granlund proposed G type descriptor (Granlund, 1972 [28]). Z type descriptor is defined as the cumulative angle changes of the contour points from the starting point is expanded with Fourier series while G type descriptor defined as the length between the contour points from the start point of contour line in concern is expanded with Fourier series. Both of descriptors have the following problems:

It is hard to express local properties,

It cannot represent the shape of contour when the shape is not closed,

The results depend on the start point on the contour line in concern for tracking.

On the other hand, Z type descriptor has another difficulty that the convergence speed is not fast so that it takes relatively large computational resources and the reproducibility of low frequency component is not good enough. Meanwhile, G type descriptor has another difficulty that Gibbs phenomenon (Gibbs, 1899 [29]) would occur at the end points of the closed curve of contour lines results in the end points cannot be preserved.

The shape descriptor proposed here is wavelet based descriptor not the Fourier type of descriptor. Therefore, the proposed wavelet based descriptor allows shape description through frequency-time analysis while Fourier based descriptor allows only frequency components representation of shape. There is some advantage for the wavelet based descriptor in shape information extraction rather than Fourier descriptor. Wavelet descriptor is proposed for best matching method to measure similarity between two feature vectors of the two shapes (Yang, et al., 1998 [30], Tieng, et al., 1997 [31]). This is impractical for higher dimensional feature matching. Therefore, wavelet descriptors are more suitable for model-based object recognition than

data-driven shape retrieval, because for shape retrieval, which is usually conducted online, speed is essential.

Contour of the object extracted from the original image can be expressed with wavelet based descriptor. The proposed image retrieval method is based on the hue information and texture as well as the proposed wavelet described shape information of extracted objects to improve image retrieval success rate.

The following section describes the proposed image retrieval method followed by some experiments for reproducibility of the proposed wavelet descriptor in comparison to the conventional Fourier descriptor with several simple symmetrical and asymmetrical shapes. Then it is validated with the image database of phytoplankton (Arai and Tearayama, 2010 [32]).

2 Proposed Method

2.1 Process Flow of the Proposed Image Classification

There are some image retrieval methods which are based on the following features,

(1) Extraction of Visual Signature,

(2) Image Similarity Using Visual Signature,

(3) Clustering and Classification,

(4) Relevance Feedback-Based Search Paradigms,

(5) Multimodal Fusion and Retrieval

Hit rate, however, is not good enough for the conventional image retrieval methods. The following features can be applicable for image retrievals,

Spectral features: intensity, color, etc.

Spatial features: shape, size, texture, etc.

Relational features: relations among image portions or segments, semantic information, knowledge based information, etc.

Hue and texture information are used as typical features for discrimination and classification Image classification method based on hue information [33] and wavelet description based shape information [34] as well as texture information of the objects extracted with dyadic wavelet transformation [35] is proposed. Object is assumed to be focused so that the frequency component in the object is relatively high in comparison to the other (background). Figure 1 shows the process flow of the proposed image classification method.

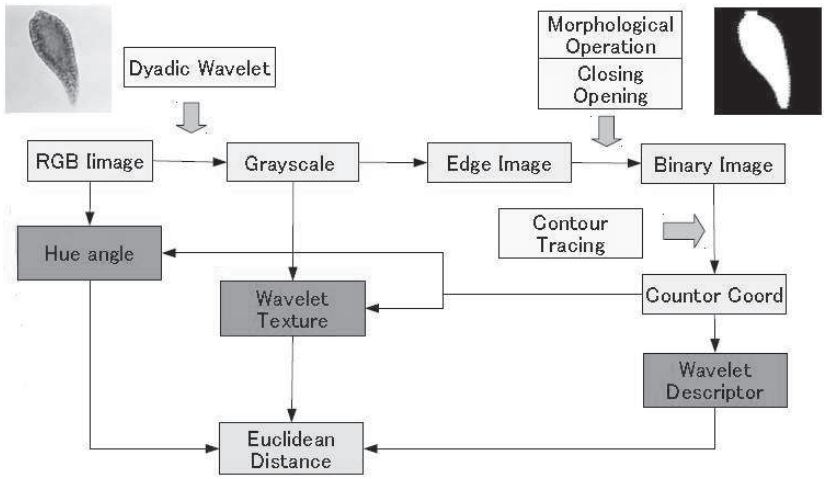

Fig. 1. Process flow of the proposed image classification method.

One of the image features of hue information (angle) is calculated for the entire image in the color image database. Dyadic wavelet transformation10 is also applied to the images then texture information is extracted from the transformed resultant image. Based on the Dyadic wavelet transformation, HH11 image of edge is extracted from the original image. Morphological operations12, opening and closing are then applied to the edge extracted images to remove inappropriate isolated pixels and undesirable image defects. After that the resultant image is binarized with appropriate threshold then contour of the object is extracted. Then the Dyadic wavelet transformation is applied to the contour in order to extract shape information (Wavelet descriptor). After all, Euclidian distance between target image and the other candidate images in the color image database is calculated with extracted hue, texture and shape information then the closest image is retrieved.

Normalization of the extracted features is applied in the proposed method. Then image in concern is retrieved with Euclidian distance between features of the image in concern and the images in the given image database. B. Dyadic wavelet transformation Using dyadic wavelet, frequency component can be detected. Dyadic wavelet allows to separate frequency components keeping image size with that of original image. Dyadic wavelet is called as a binary wavelet and has high pass and low pass filter components, $\{h[k], g[k]\}$ and reconstruction filter $\{h[k], g[k]\}$. Low and high frequency components, Cn and dn are expressed as follows,

$$Cn\,[i]=\Sigma k\; h[k\,]Cn-1\;[i+k2n-1\,] \tag{1}$$

$$dn\,[i]=\Sigma k\; g\,[k\,]Cn-1\;[i+k2n-1\,] \tag{2}$$

Then original image is also reconstructed with the low and high frequency components as follows,

$$Cn-1\;[i]=1/2\;\Sigma k\; h[k\,]Cn[i-k2n-1]+\Sigma k\; g[k\,]dn\;[i-k2n-1\,] \tag{3}$$

If a new parameter s[m] is employed, then lifting dyadic wavelet is defined as follows,

$$hnew[k\,]=hold\,[k\,] \tag{4}$$

$$hnew[k\,]=hold\,[\,k\,]+\Sigma m\; s[-m]\; g\; old\;[k-m] \tag{5}$$

$$gnew[k\,]=gold\,[\,k\,]-\Sigma m\; s[m]\; hold\,[\,k-m] \tag{6}$$

$$gnew[k\,]=g\; old\;[k\,] \tag{7}$$

2.2 Dyadic wavelet based descriptor (Shape information)

Image classification method with hue and texture information is conventional. In the proposed method, another feature, shape information is employed. Fourier descriptor is used, in general, to represent shape information. Although Fourier descriptor represents frequency component of the contour line, location information cannot be described. In other words, Fourier descriptor does support only frequency analysis, and does not support time-frequency component analysis. Wavelet descriptor which is proposed by this

paper supports a time-frequency component analysis so that not only frequency component but also location of contour edge can be discussed [36].

Let *u(i)* be distance between a point in the closed object contour line and a certain point i on the line, then the closed object contour line can be represented as *u(i), i*=1,2,…,*n. i*=1 corresponds to 0 degree while *i*=*n* corresponds to 360 degree, respectively as shown in Figure 2.

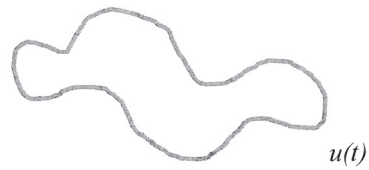

Fig.2 Example of extracted contour of the object in concern

u(i) can be converted with dyadic wavelet transformation. Then the contour line can be represented with high frequency component of the dyadic wavelet transformed sequence as is shown in Figure 3. Then average of the high frequency component of pixel value is used for a feature of the image classification. The contour line can be represented with high frequency component of the dyadic wavelet transformed sequence, Then average of the high frequency component of pixel value is used for a feature of the image retrieval.

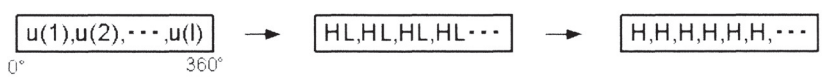

Contour locations Wavelet transformation

Reconstruction

Fig. 3. Dyadic wavelet descriptor for representation of the closed object contour lines.

Wavelet analysis makes available a time-frequency analysis so that influence due to start point dependency can be eliminated. It can represent the detailed shape in particular local shape with 2x2 of wavelet transformation. It is easy to implement wavelet descriptor because only thing user has to do is replace

Fourier transformation to wavelet transformation (Dyadic wavelet in the proposed method).

Alternative shape information is Fourier Descriptor. Zahn and Roskies proposed Z type descriptor while Granlund proposed G type descriptor. These are as follows,

Z type descriptor: Cumulative angle changes of the contour points from the starting point is expanded with Fourier series

G type descriptor: length between the contour points from the start point of contour line in concern is expanded with Fourier series

The location coordinate is expressed in the complex plane representation for the G type of Fourier descriptor, that is,

$$Z_s = X_s + iY_s \tag{8}$$

Then space or time domain locations can be transformed with eth following equation,

$$F_t = \frac{1}{S}\sum_{s=0}^{S-1} Z_s \exp\left(\frac{-2\pi ks}{S} i\right) \tag{9}$$

It can be inversely transformed with the following equation,

$$Z_s = \sum_{t=0}^{S-1} F_t \exp\left(\frac{2\pi ks}{S} i\right) \tag{10}$$

Namely, the location coordinate is expressed in the complex plane representation.

Both of descriptors has the following problems It is hard to express local properties. It cannot represent the shape of contour when the shape is not closed. The results depend on the start point on the contour line in concern for tracking. Other than these, both descriptors have their following specific problems,

Z type descriptor: Convergence speed is not fast so that it takes relatively large computational resources, also Reproducibility of low frequency component is not good enough

G type descriptor: Gibbs phenomenon would occur at the end points of the closed curve of contour lines results in the end points cannot be preserved

2.3 Texture information

Also texture information is useful for discrimination. Texture information can be derived from dyadic wavelet transformation. Texture information is defined as high frequency component of pixel value derived from dyadic wavelet transformation. Daubechies wavelet transformation is applied to the 2x2 pixels defined in Figure 4.

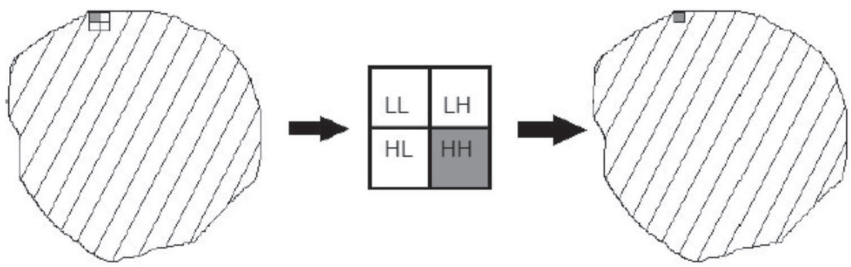

Fig.4. Detected object and 2x2 of matrix in the object to detect texture information with 2x2 of dyadic wavelet transformation.

Pixel value of the pixel in the object is replaced to the high frequency component detected with Daubechies wavelet. Thus image which represents texture information of the detected object image is generated [37]. Daubechies base function of wavelet has order. 1st order of Daubechies base function is totally equal to Haar base function. In this paper, 1st, 2nd,4th order of Daubechies base function is used and compare their classification and image retrieval performance with Euclidean distance between the specified phytoplankton and the others.

2.4 Hue angle

Thus contour of the object is detected. Then Red, Green, and Blue: RGB of the original object image can be transformed to Hue, Saturation, and Intensity: HSV information. Hue information in unit of radian, in particular, is useful for discrimination of the target image classifications of phytoplankton images.

RGB to HSV conversion is also be expressed as follows,

$V = \max(R, G, B)$

$S = (V - X)/V$ where $X = \min(R, G, B)$

$R = V: H = (\pi/3)(b - g)$

$G = V: H = (\pi/3)(2 + r - b)$

$B = V: H = (\pi/3)(4 + g - r)$

where $r = (V - R)/(V - X)$, $g = (V - G)/(V - X)$, $b = (V - B)/(V - X)$, H ranges from 0 to 360, S ranges from 0 to 1, V ranges from 0 to 1, HSV representation and R, G, B also range from 0 to 1 as shown in Figure 5.

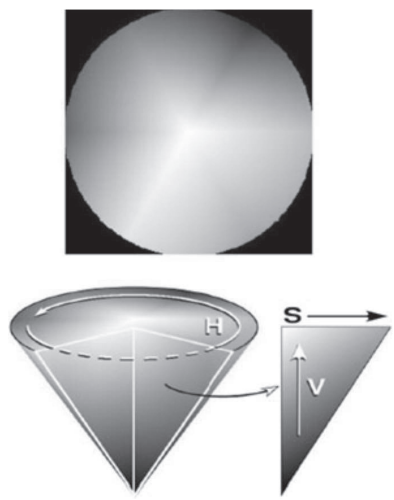

Fig.5 Color representation

These three features, hue, H, texture, *xx* and shape information, *yy* composes three dimensional feature space results in measurement of Euclidian distance between a query image and the images in previously created image database.

Using the distance, a query image can be retrieved from the image in the database. Thus image classifications can be done with hue and texture information as well as shape information derived from dyadic wavelet descriptor.

2.5 Preliminary experiment

If these transformation and inverse transformation is perfect, then the original shapes are completely reproduced. The reproducibility for the shapes of circle, triangle, square, and trapezium (asymmetric shape) of the proposed wavelet descriptor is better than that of the conventional Fourier descriptor as shown in Figure 6.

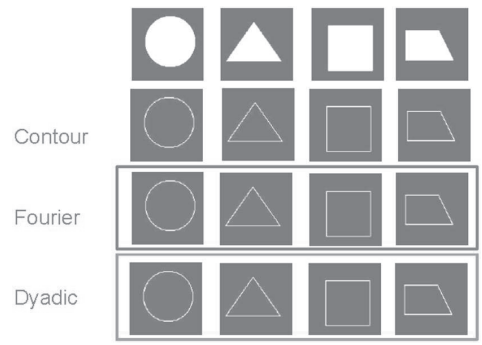

Fig.6 Comparison of reproducibility of the shapes between Fourier and Dyadic wavelet descriptor.

The process flow of the preliminary experiment is shown in Figure 7. The extracted contour is described with Fourier and wavelet descriptor. Then, contour is reconstructed with the representations of contour with Fourier and wavelet descriptors. After that, Root Mean Square; RMS error between the reconstructed counter and the original contour is calculated。

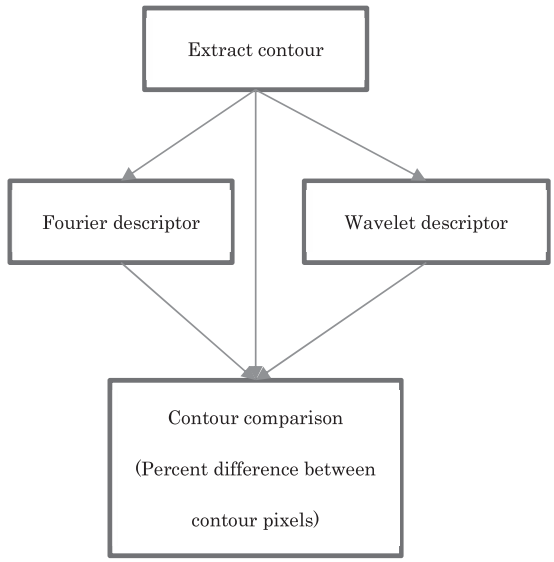

Fig.7 Process flow of the preliminary experiment

In the comparison, the original image is binarized and the contour is extracted. Then shape information is extracted with both Fourier descriptor (G-type) and Dyadic wavelet descriptor. After that, image is reconstructed with the extracted shape information then compares the reconstructed images with two descriptors, Fourier and Dyadic wavelet descriptors. The difference between the reconstructed contours and original image is shown in Table 1. Thus it is found that the reproducibility of Dyadic wavelet descriptor is better than the conventional Fourier descriptor.

TABLE 1 COMPARISON OF THE DIFFERENCE BETWEEN THE ORIGINAL AND RECONSTRUCTED CONTOURS WITH FOURIER AND DYADIC WAVELET DESCRIPTORS.

Shape		Fourier	Dyadic
circle	0.4121	0.1809	
triangle	0.5391	0.1280	
square		0.3689	0.1101
trapezium	0.4660	0.1929	

This method can be expanded to 3D object. Once 3D object image is acquired through scanning in roll/pitch/yaw directions with the appropriate step angle, and then contour lines of the acquired 2D images are extracted. After that, the 3D object shape complexity is represented with the wavelet descriptor as a resultant image which includes series of the high frequency components derived from dyadic wavelet transformation as shown in Figure 3 as shown in the following sequence,

HH..H(for roll angle 0), HH..H(for roll angle 10),.., HH..H(for roll angle 350),

HH..H(for pitch angle 0), HH..H(for pitch angle 10),.., HH..H(for pitch angle 350),

HH..H(for yaw angle 0), HH..H(for yaw angle 10),.., HH..H(for yaw angle 350). It is an image and is totally visual. This image represents 3D object shape complexity as an index. Also this index is shift invariant and rotation invariant. Namely, the index is not changed even if 3D object is translated and rotated.

3 Experiment

3.1 Data Used

Figure 8 shows intensive study area of Ariake bay in Kyushu, Japan and example of chlorophyll-a concentration derived from Terra/MODIS of remote sensing satellite.

(a)Intensive study area

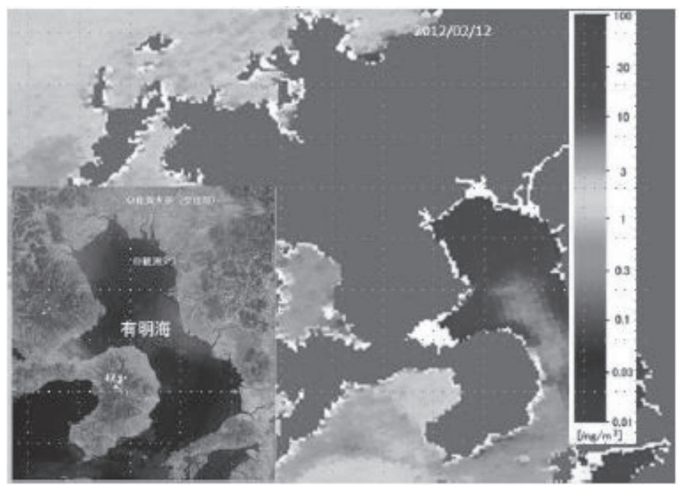

(b)Example of Chlorophyll-a concentration image derived from Terra/MODIS sensor

Fig.8 Intensive study area of Ariake bay and chlorophyll-a concentration in unit of $\mu g/m^3$

Ariake Bay is a portion of Ariake Sea of which the width is around 20km (in direction of east to west) and the length is approximately 100km (in direction of north to south). It is almost closed sea area because the mouth of Ariake

Sea is quite narrow. Sea water exchanges are, therefore, very small. Diatom blooms have recurrently appeared from late autumn to early spring in the coastal waters of western Japan, such as the Ariake Bay and the Seto Inland Sea, where large scale "Nori" aquaculture occurs.

Red tide is a severe problem not only for fisherman, but also for ocean biologists. Red tide occurs in a nutrient-rich ocean, chlorophyll-a rich ocean results in photosynthesis is getting active. Red tide is one of indicators for ocean healthiness.

Nutrition-rich water makes chlorophyll-a increasing phytoplankton and thus red tide occurs.

Diatom blooms have caused the exhaustion of nutrients in the water column during the "Nori" harvest season. The resultant lack of nutrients has suppressed the growth of "Nori" and lowered the quality of "Nori" products due to bleaching with the damage of the order of billions of Japanese yen (Approx.25 billion yen for Ariake Bay).

This example of the MODIS derived chlorophyll-a concentration which are acquired on February 12 2012. The Ariake Sea is the largest productive area of Nori (Porphyra yezoensis1) in Japan. In winters in 2012, 2013, 2014 and 2015, as well as 2016, a massive diatom bloom appeared in the Ariake Bay, Japan. In case of above red tides, bloom causative was *Rhizosolenia imbricate*2 and *Eucampia zodiacus*. This bloom has been occurred several coastal areas in Japan and is well reported by Nishikawa et al. for Harima-nada sea areas. Diatom blooms have recurrently appeared from late autumn to early spring in the coastal waters of western Japan, such as the Ariake Bay and the Seto Inland Sea, where large scale "Nori" aquaculture occurs. Diatom blooms have caused the exhaustion of nutrients in the water column during the "Nori" harvest season. The resultant lack of nutrients has suppressed the growth of "Nori" and lowered the quality of "Nori" products due to bleaching with the damage of the order of billions of Japanese yen.

There are a plenty of red tide species. Small portion of red tide species can be listed up in Figure 9. These red tide species can be classified into three

categories, (a) Caution level of species, (b) Warning level of species, and (c) Dangerous species. Fishes and shells take these dangerous red tide species.

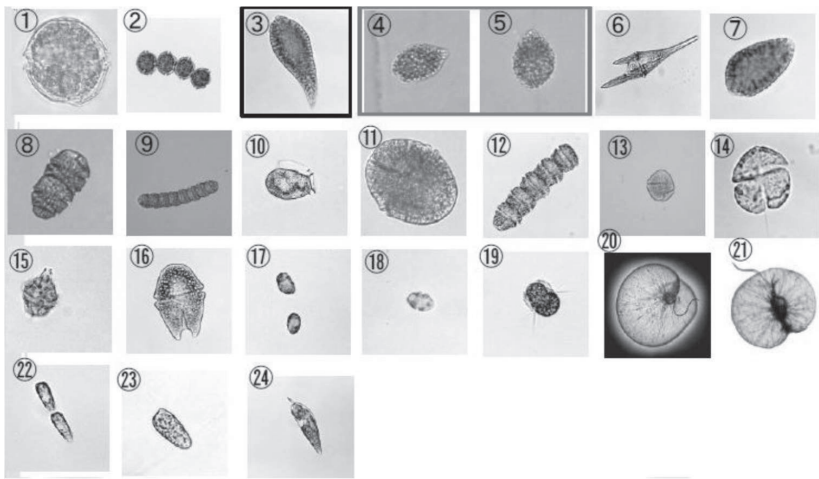

Fig.9 Photos of a portion of red tide species

After that human habitats eat the fishes and shells. Then such persons get a bad situation and have an illness condition. Therefore, these red tide species are classified into dangerous species. Identifying these dangerous red tide species is important. It, however, is not so easy to classify because these three categories of red tide species are quite resemble. Usually, the local fishery research institutes measure red tide from the research vessels with microscope. They used to count the number of red tide with microscope camera acquired imagery data on the ship. Then identify the red tide species in the same time quickly. Even though human perception capability is superior to that by machine learning based automatic classification, there are some mistakes. The purpose of the research is to improve classification performance by using considerable features which can be extracted from the microscopic imagery data.

Figure 10 shows the extracted edges of the phytoplankton shapes.

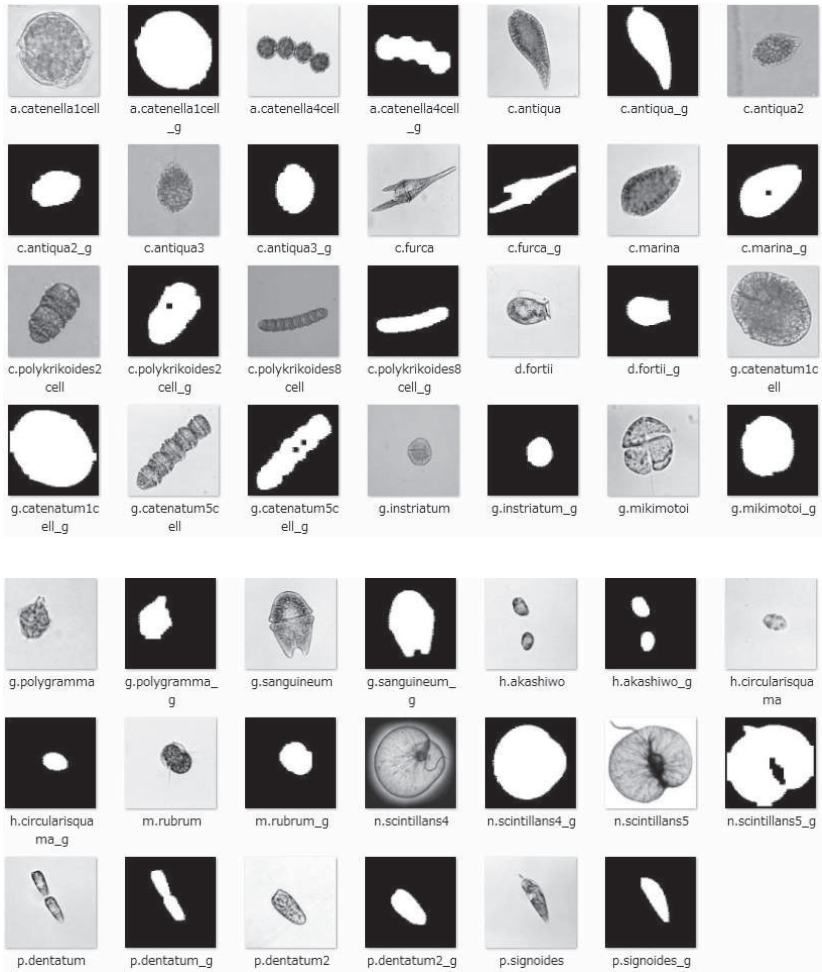

Fig.10 Extracted edges of the phytoplankton shapes.

3.2 Comparison of Euclidian Distance Between *Cahttnella Antiqua-3* and the Others with Three Features, Texture, Hue and Wavelet Discriptor Based on Daubechies 1, 2, and 4

One of the measures for classification performance evaluation is Euclidian distance among the classes in concern. Shorter Euclid distance implies a poor classification performance while longer distance means a good performance.

Euclid distance between *Chattnella_Antiqua-3* and the other species are calculated and shown in Table 2, 3, 4 for the case of utilizing all these three features of wavelet descriptor with Daubechies 1, 2, and 4, respectively.

Calculated Euclid Distance when Texture Wavelet Descripter and hue information are used as features.

TABLE 2. EUCLID DISTANCE BETWEEN CHATTNELLA ANTIQUA3 AND THE OTHERS WITH DAUBECHIES 1

Daubechies 1	Mean				Normalized Mean		Euclid Distance		
wavelet	texture	hue(rad)	wavelet	texture	hue(rad)	Normalized		Mean	%Improve
a.catenella1cell	0.196484	4.320291	1.29206	4.320291	5.208882	3.47149	2.610026	0.730394	257.3451
a.catenella4cell	0.263178	5.48481	3.647233	5.48481	12.68603	5.002298	8.867848	3.258216	172.1688
c.antiqua	0.283669	5.571536	0.892777	5.571536	3.941248	5.472623	1.887694	1.870292	0.930425
c.antiqua2	0.288699	3.577128	2.054994	3.577128	7.631026	5.588075	3.60677	1.141521	215.9618
c.antiqua3	0.29426	3.701602	0.920312	3.701602	4.028665	5.715715	0	0	0
c.furca	0.246901	8.065513	1.742646	8.065513	6.639391	4.628697	5.200117	4.440745	17.1001
c.marina	0.222682	3.65	0.779962	3.65	3.583085	4.072805	1.703043	0.183073	830.2522
c.polykrikoides2cell	0.24923	3.70454	1.181714	3.70454	4.858558	4.682154	1.325511	0.271051	389.0264
c.polykrikoides8cell	0.217637	3.961787	1.173258	3.961787	4.831712	3.957009	1.950802	0.364634	435.0023
d.fortii	0.327144	9.655471	1.421595	9.655471	5.620126	6.470492	6.208945	5.975446	3.90763
g.catenatum1cell	0.210512	4.233059	0.83791	4.233059	3.767057	3.79347	2.011445	0.544842	269.1797
g.catenatum5cell	0.230301	8.044559	0.789282	8.044559	3.612674	4.247682	4.603199	4.345976	5.918657
g.instriatum	0.411956	4.286565	1.57805	4.286565	6.116836	8.417158	3.464165	0.896759	286.2983
g.mikimotoi	0.256012	5.721647	2.321516	5.721647	8.477174	4.837819	4.963921	2.459018	101.866
g.polygramma	0.295303	7.345761	1.019077	7.345761	4.342222	5.739655	3.657702	3.645502	0.334673
g.sanguineum	0.27297	9.884615	1.184978	9.884615	4.86892	5.227051	6.258951	6.188811	1.13334
h.akashiwo	0.550117	7.972222	0.993822	7.972222	4.262043	11.58833	7.265003	4.2888	69.39478
h.circularisquama	0.499699	4.288433	0.850071	4.288433	3.805666	10.4311	4.756989	0.665326	614.9864
m.rubrum	0.35107	7.850218	1.444111	7.850218	5.69161	7.019659	4.655821	4.182799	11.30874
n.scintillans4	0.225198	3.990742	2.205616	3.990742	8.109217	4.130554	4.387168	1.320164	232.3199
n.scintillans5	0.184937	2.872873	1.507892	2.872873	5.8941	3.206455	3.23466	1.026171	215.2166
Mean	0.289427	5.62778	1.420899	5.62778	5.617916	5.604776	3.934275	2.276169	196.6501
Standard Deviation	0.095136	2.183621	0.687803	2.183621	2.183621	2.183621	2.147732	1.994634	224.5983

TABLE 3. EUCLID DISTANCE BETWEEN *CHATTNELLA ANTIQUA3* AND THE OTHERS WITH DAUBECHIES 2

Daubechies 2		Mean		Normalized Mean			Euclid Disatance		
wavelet	texture	hue(rad)	wavelet	texture	hue(rad)		Normalized	Mean	%Improve
a.catenella1cell	0.080995	4.320291	1.29206	4.320291	5.208882	3.705773	2.32756	0.730394	218.672
a.catenella4cell	0.170238	5.48481	3.647233	5.48481	12.68603	5.416414	8.841316	3.258216	171.3545
c.antiqua	0.155219	5.571536	0.892777	5.571536	3.941248	5.128525	1.933937	1.870292	3.402932
c.antiqua2	0.171255	3.577128	2.054994	3.577128	7.631026	5.435908	3.608915	1.141521	216.1497
c.antiqua3	0.180553	3.701602	0.920312	3.701602	4.028665	5.614136	0	0	0
c.furca	0.159615	8.065513	1.742646	8.065513	6.639391	5.212789	5.101048	4.440745	14.86918
c.marina	0.085888	3.65	0.779962	3.65	3.583085	3.799564	1.869191	0.183073	921.0066
c.polykrikoides2cell	0.117673	3.70454	1.181714	3.70454	4.858558	4.40883	1.463384	0.271051	439.8925
c.polykrikoides8cell	0.147278	3.961787	1.173258	3.961787	4.831712	4.976309	1.058019	0.364634	190.1588
d.fortii	0.236693	9.655471	1.421595	9.655471	5.620126	6.690247	6.256143	5.975446	4.697494
g.catenatum1cell	0.103167	4.233059	0.83791	4.233059	3.767057	4.130774	1.597262	0.544842	193.1609
g.catenatum5cell	0.098365	8.044559	0.789282	8.044559	3.612674	4.038728	4.63856	4.345976	6.732285
g.instriatum	0.315118	4.286565	1.57805	4.286565	6.116836	8.193524	3.369849	0.896759	275.781
g.mikimotoi	0.122712	5.721647	2.321516	5.721647	8.477174	4.505419	5.009897	2.459018	103.7357
g.polygramma	0.16845	7.345761	1.019077	7.345761	4.342222	5.382141	3.664974	3.645502	0.534143
g.sanguineum	0.134972	9.884615	1.184978	9.884615	4.86892	4.740423	6.300718	6.188811	1.808221
h.akashiwo	0.503999	7.972222	0.993822	7.972222	4.262043	11.81406	7.532047	4.2888	75.62133
h.circularisquama	0.429245	4.288433	0.850071	4.288433	3.805666	10.38115	4.808173	0.665326	622.6794
m.rubrum	0.260962	7.850218	1.444111	7.850218	5.69161	7.155443	4.727793	4.182799	13.02941
n.scintillans4	0.105809	3.990742	2.205616	3.990742	8.109217	4.181417	4.334419	1.320164	228.3243
n.scintillans5	0.053063	2.872873	1.507892	2.872873	5.8941	3.170363	3.184127	1.026171	210.2921
Mean	0.181013	5.62778	1.420899	5.62778	5.617916	5.622949	3.887016	2.276169	186.2811
Standard Deviation	0.113918	2.183621	0.687803	2.183621	2.183621	2.183621	2.233389	1.994634	233.1855

TABLE 4. EUCLID DISTANCE BETWEEN *CHATTNELLA ANTIQUA3* AND THE OTHERS WITH DAUBECHIES 4

Daubechies 4	Mean	Normalized Mean	Euclid Disatance

wavelet	texture	hue(rad)	wavelet	texture	hue(rad)	Normalized	Mean	%Improve
a.catenella1cell	0.088846	4.320291	1.29206	4.320291	5.208882	3.698761	2.237914	0.730394	206.3984
a.catenella4cell	0.194141	5.48481	3.647233	5.48481	12.68603	5.391889	8.839726	3.258216	171.3057
c.antiqua	0.176529	5.571536	0.892777	5.571536	3.941248	5.10869	1.911765	1.870292	2.217423
c.antiqua2	0.192126	3.577128	2.054994	3.577128	7.631026	5.359488	3.607122	1.141521	215.9926
c.antiqua3	0.200659	3.701602	0.920312	3.701602	4.028665	5.496697	0	0	0
c.furca	0.184336	8.065513	1.742646	8.065513	6.639391	5.234226	5.092004	4.440745	14.66552
c.marina	0.095042	3.65	0.779962	3.65	3.583085	3.798392	1.756543	0.183073	859.4753
c.polykrikoides2cell	0.129042	3.70454	1.181714	3.70454	4.858558	4.345107	1.419469	0.271051	423.6906
c.polykrikoides8cell	0.164878	3.961787	1.173258	3.961787	4.831712	4.921344	1.021573	0.364634	180.1637
d.fortii	0.278876	9.655471	1.421595	9.655471	5.620126	6.754414	6.289925	5.975446	5.26285
g.catenatum1cell	0.113391	4.233059	0.83791	4.233059	3.767057	4.093441	1.523159	0.544842	179.5599
g.catenatum5cell	0.105457	8.044559	0.789282	8.044559	3.612674	3.965864	4.623611	4.345976	6.388313
g.instriatum	0.372052	4.286565	1.57805	4.286565	6.116836	8.25267	3.506854	0.896759	291.0587
g.mikimotoi	0.147609	5.721647	2.321516	5.721647	8.477174	4.643661	4.959585	2.459018	101.6897
g.polygramma	0.194853	7.345761	1.019077	7.345761	4.342222	5.403337	3.658815	3.645502	0.365202
g.sanguineum	0.15963	9.884615	1.184978	9.884615	4.86892	4.836957	6.274626	6.188811	1.386621
h.akashiwo	0.588219	7.972222	0.993822	7.972222	4.262043	11.7286	7.558393	4.2888	76.23562
h.circularisquama	0.506198	4.288433	0.850071	4.288433	3.805666	10.40972	4.952965	0.665326	644.442
m.rubrum	0.302785	7.850218	1.444111	7.850218	5.69161	7.138867	4.76163	4.182799	13.83836
n.scintillans4	0.11566	3.990742	2.205616	3.990742	8.109217	4.129926	4.31307	1.320164	226.7071
n.scintillans5	0.0558	2.872873	1.507892	2.872873	5.8941	3.167387	3.097148	1.026171	201.8161
Mean	0.207911	5.62778	1.420899	5.62778	5.617916	5.613306	3.876471	2.276169	182.0314
Standard Deviation	0.135799	2.183621	0.687803	2.183621	2.183621	2.183621	2.255699	1.994634	225.2163

It is clear that the mean and standard deviation after the normalization are same in comparison to the before the normalization. It also found that the Euclidian distance between *Chattnella Antiqua-3* and the others are improved remarkably, around twice much longer distance.

3.3 Euclidian Distance Between *Chattnella Antica-3* and the Others Using Hue and Texture information as well as with and without Wavelet Discriptor

Effectiveness of the wavelet descriptor is evaluated through comparisons of Euclidian distance between *Chattnella Antiqua-3* of specie and the other species calculated with the normalized features. Table 5, 6, 7 shows the results for Daubechies 1, 2, 4 of base function of wavelet.

The mean of Euclidian distance for without wavelet descriptor shows around 2.7 while that with wavelet descriptor shows more than 3.8. Therefore, effectiveness of wavelet descriptor is corresponding to 40% improvement of Euclidian distance which results in40 % improvement of image retrieval and classification.

TABLE 5. EUCLID DISTANCE BETWEEN *CHATTNELLA ANTIQUA3* AND THE OTHERS WITH DAUBECHIES 1

Daubechies 1 Wavelet Descriptor	With	Without
a.catenella1cell	2.610026	2.535638
a.catenella4cell	8.867848	8.686708
c.antiqua	1.887694	0.258332
c.antiqua2	3.60677	3.604622
c.antiqua3	0	0
c.furca	5.200117	2.827985
c.marina	1.703043	1.702262
c.polykrikoides2cell	1.325511	1.325508
c.polykrikoides8cell	1.950802	1.933373
d.fortii	6.208945	1.761374
g.catenatum1cell	2.011445	1.939965
g.catenatum5cell	4.603199	1.525834
g.instriatum	3.464165	3.414419
g.mikimotoi	4.963921	4.534306

g.polygramma	3.657702	0.314469
g.sanguineum	6.258951	0.972019
h.akashiwo	7.265003	5.87725
h.circularisquama	4.756989	4.720654
m.rubrum	4.655821	2.11321
n.scintillans4	4.387168	4.37763
n.scintillans5	3.23466	3.126697
Mean	3.934275	2.740584
Standard Deviation	2.147732	2.077256

TABLE 6. EUCLID DISTANCE BETWEEN CHATTNELLA ANTIQUA3 AND THE OTHERS WITH DAUBECHIES 2

Daubechies 2 Wavelet Descriptor	With	Without
a.catenella1c ell	2.3275 6	2.24382 7
a.catenella4c ell	8.8413 16	8.65962 1
c.antiqua	1.9339 37	0.49341 6
c.antiqua2	3.6089 15	3.60676 7
c.antiqua3	0	0
c.furca	5.1010 48	2.64139 6
c.marina	1.8691 91	1.86847 8
c.polykrikoid es2cell	1.4633 84	1.46338 1
c.polykrikoid es8cell	1.0580 19	1.02552 8

d.fortii	6.2561	1.92113
	43	6
g.catenatum1	1.5972	1.50625
cell	62	4
g.catenatum5	4.6385	1.62940
cell	6	4
g.instriatum	3.3698	3.31869
	49	
g.mikimotoi	5.0098	4.58459
	97	2
g.polygramm	3.6649	0.39005
a	74	
g.sanguineu	6.3007	1.21218
m	18	9
h.akashiwo	7.5320	6.20431
	47	6
h.circularisq	4.8081	4.77222
uama	73	7
m.rubrum	4.7277	2.26738
	93	
n.scintillans4	4.3344	4.32476
	19	5
n.scintillans5	3.1841	3.07439
	27	
Mean	3.8870	2.72418
	16	1
Standard	2.2333	2.09672
Deviation	89	8

TABLE 7. EUCLID DISTANCE BETWEEN CHATTNELLA ANTIQUA3 AND THE OTHERS WITH DAUBECHIES 4

Daubechies 4 Wavelet Descriptor	With	Without
a.catenella1cell	2.237914	2.150694
a.catenella4cell	8.839726	8.657998
c.antiqua	1.911765	0.397732
c.antiqua2	3.607122	3.604973
c.antiqua3	0	0
c.furca	5.092004	2.623887
c.marina	1.756543	1.755785
c.polykrikoides2cell	1.419469	1.419465
c.polykrikoides8cell	1.021573	0.987884
d.fortii	6.289925	2.028448
g.catenatum1cell	1.523159	1.427433
g.catenatum5cell	4.623611	1.586348
g.instriatum	3.506854	3.457722
g.mikimotoi	4.959585	4.529559
g.polygramma	3.658815	0.32716
g.sanguineum	6.274626	1.06831
h.akashiwo	7.558393	6.236273
h.circularisquama	4.952965	4.918078
m.rubrum	4.76163	2.337115
n.scintillans4	4.31307	4.303367
n.scintillans5	3.097148	2.984214
Mean	3.876471	2.704878
Standard Deviation	2.255699	2.126147

3.4 Euclidian distance between query image and the image in the image database

In order to show the effectiveness of the wavelet descriptor based shape complexity feature, just three dimensional feature spaces is used because small dimensionality is much comprehensive. In the feature space, the aforementioned three features, hue (H) which is the averaged hue in unit of

radian over the object area, wavelet descriptor (W) which is the averaged high frequency component of pixel value along with the contour line of the object and Texture (T) which is the averaged high frequency of pixel value over the object area are used to discriminate the object included images thus image retrieval is made by using a distance between location of the current image and locations of the previously acquired images in the feature space. As it is aforementioned, Hue, texture, and shape information are scalar value and these features become a vector in the feature space. From an image in image DB, three features are extracted and the image becomes a vector in the three dimensional feature spaces. Figure 11 shows the distance between *Chatnella Antiqua* of phytoplankton and the other phytoplankton. Figure 11 (a) shows the distance in case of texture information only while Figure 11 (b) shows that for hue information. Meanwhile, Figure 11 (c) and (d) shows that of Dyadic wavelet and Fourier descriptors, respectively. On the other hand, Figure 11 (e) shows that when hue, texture and Dyadic wavelet descriptor is used while Figure 11 (f) shows that hue, texture and Fourier descriptor is used.

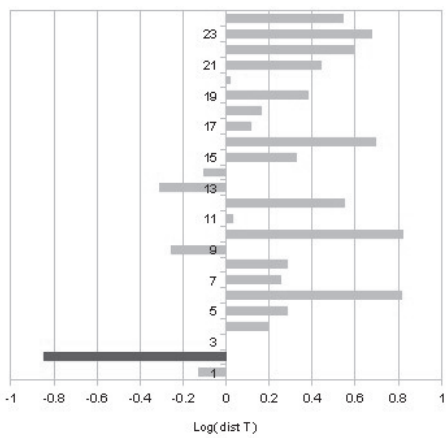

(a) Texture

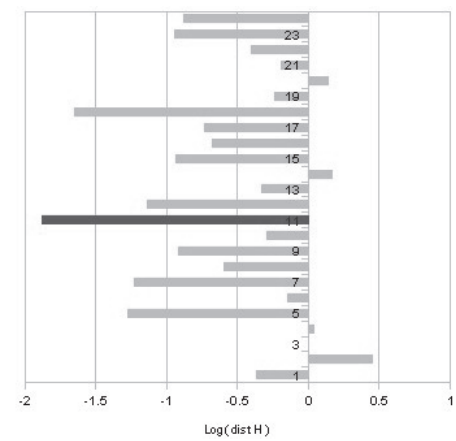

(b) Hue

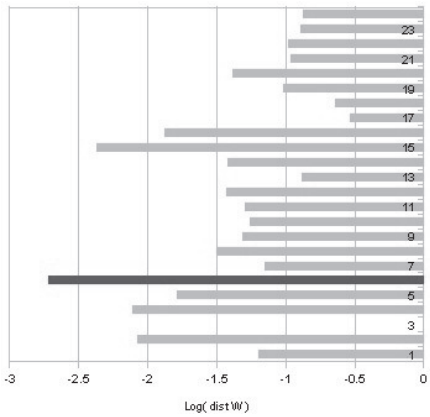

(c) Wavelet descriptor

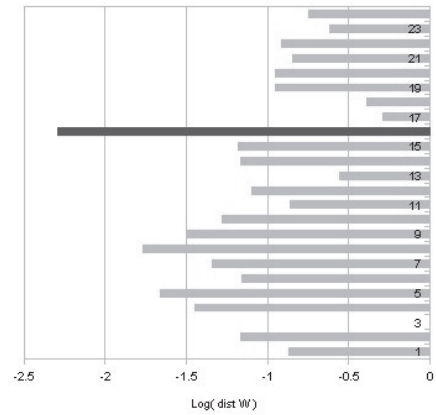

(d) Fourier descriptor

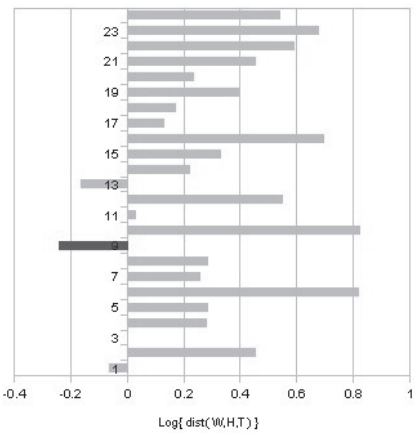

(e) Wavelet descriptor + Hue + Texture

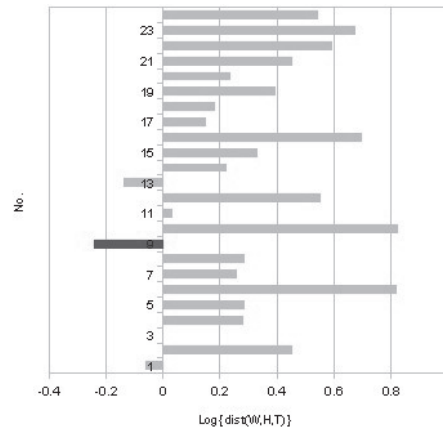

(f) Fourier descriptor + Hue + Texture

Fig.10 Comparisons between *Chattnella Antiqua* and the closest phytoplankton in the Euclidian feature space.

The distance for both cases using hue and texture only is too short so that separability is not good enough in comparison to the shape information with Fourier or wavelet descriptors. The distance of the hue is twice much longer than that of texture. Although the texture of the phytoplankton is very similar, colors of phytoplankton are different. Shape information based distance is a little bit longer than that of hue as well as texture information. When hue, texture, and shape information are used, the distance between Dyadic wavelet and Fourier descriptors together with hue and texture is very similar.

Figure 12 shows scatter diagram of phytoplankton species with the vertical axis is Wavelet descriptor. Taking *Chattonella Antiqua* of phytoplankton as a query image, Euclidian distance between the query image and the others are calculated. The distance calculated with the features of hue and texture only is shown in Table 8 while Table 9 shows the distance with the feature of wavelet descriptor, hue and texture.

Euclidian distance between *Chattonella Antiqua* and the others ranges from 0.005 to 11.52 for the features of hue and texture only while that ranges from 0.24 to 3.40. Table 3 shows rating results of Euclidian distance between *Chattonella Antiqua* and the others and averaged Euclidian distance between both. The averaged Euclidian distance between *Chattonella Antiqua* and the others with the feature of hue and texture only is shorter than that with feature of hue, texture and wavelet descriptor of shape information.

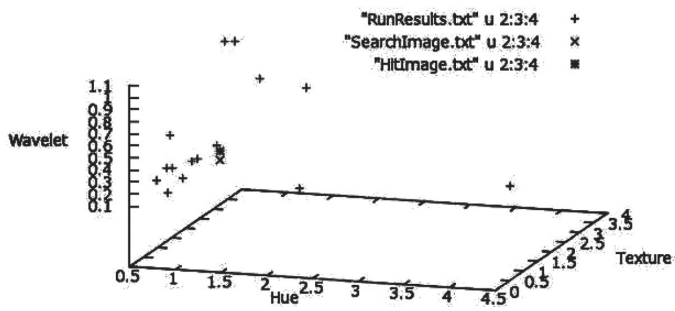

(a)

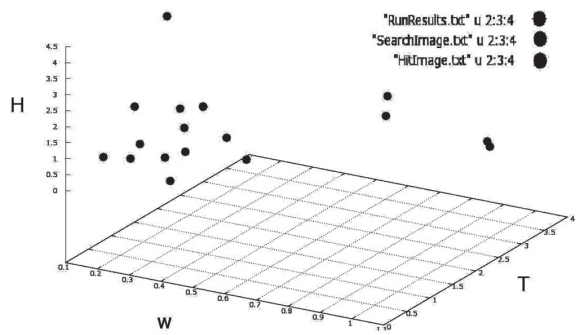

(b)

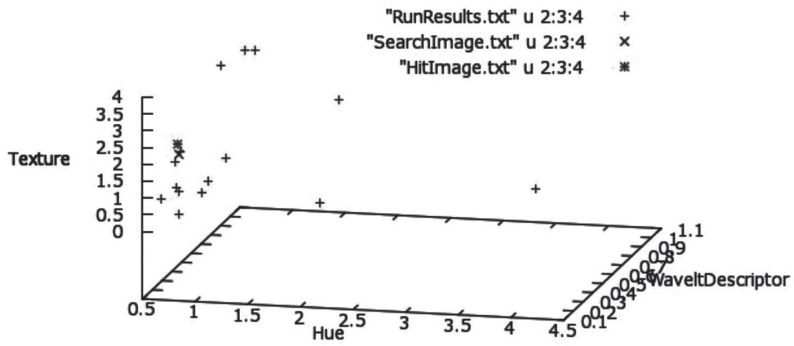

(c)

Fig.11. The feature space consists of hue (H), wavelet descriptor (W) and texture (T) for image retrievals (vertical axis is Wavelet descriptor).

TABLE 8 EUCLIDIAN DISTANCE BETWEEN *CHATTONELLA ANTIQUA* AND THE OTHERS WITH FEATURES OF HUE AND TEXTURE ONLY.

Phytoplankton	Hue	Texture	Distance
c.antiqua4	2.21	0.81	-
g.polygramma	2.42	0.75	0.05
g.catenatum	1.77	0.70	0.25
d.fortii	1.43	1.01	0.64
mesodinium_rubrum	1.37	0.52	0.78
c.antiqua3	2.26	1.74	0.87
heterosigma_akashiwo2	2.95	0.64	0.58
heterosigma_akashiwo	2.98	0.74	0.60
heterocapsa_circularisquama	0.10	0.77	1.46
g.catenatum2	0.91	0.90	0.01
c.antiqua	0.83	0.65	1.93
noctiluca_scintillans	0.72	0.58	2.29
cochlodinium_polykrikoides2cell	3.66	0.80	2.11
p.signoides	0.50	0.82	2.93
p.dentatum	0.41	0.79	3.25
gymnodinium_mikimotoi	0.85	2.10	3.52
a.catenella	1.64	4.16	11.52

TABLE 9 EUCLIDIAN DISTANCE BETWEEN *CHATTONELLA ANTIQUA* AND THE OTHERS WITH FEATURES OF WAVELET DESCRIPTOR, HUE AND TEXTURE.

Phytoplankton	Hue	Texture	Wavelet	Distance
c.antiqua4	0.144	2.21	0.81	-
g.polygramma	0.18	2.42	0.75	0.24
g.catenatum	0.22	1.77	0.70	0.45
d.fortii	0.40	1.43	1.01	0.84
mesodinium_rubrum	0.47	1.37	0.52	0.94
c.antiqua3	0.78	2.26	1.74	1.13
heterosigma_akashiwo2	1.01	2.95	0.63	1.15
heterosigma_akashiwo	1.00	2.98	0.74	1.15
heterocapsa_circularisquama	0.19	1.00	0.77	1.21
g.catenatum2	0.35	0.91	0.90	1.32
c.antiqua	0.29	0.83	0.65	1.40
noctiluca_scintillans	0.20	0.71	0.58	1.51
cochlodinium_polykrikoides2cell	0.58	3.66	0.80	1.52
p.signoides	0.36	0.50	0.82	1.73
p.dentatum	0.16	0.41	0.79	1.80
gymnodinium_mikimotoi	0.19	0.85	2.10	1.88
a.catenella	0.18	1.64	4.16	3.40

.Table 10 shows average of the features, hue, texture, and shape information with descriptors, Dyadic wavelet descriptor and Fourier descriptor as well as the percent difference between both. The proposed Dyadic wavelet descriptor shows the most significant difference between both, 22.59%. It is almost 3.8 times in comparison to the conventional Fourier descriptor. Also Euclidean distance between both in the case of hue, texture, and Dyadic wavelet descriptor is 0.5751 while that of Fourier descriptor is 0.5739 results in 0.21% improvement is achieved with the proposed Dyadic wavelet descriptor in terms of distance in the feature space which consists of hue, texture, and shape information of features. It depends on the weights for each feature. If the weight for Dyadic wavelet is set as much as large in comparison to the others,

then much longer distance can be achieved. In the case of equal weight for all three features, the distance shown in Table 11 can be achieved. If the weight for Dyadic wavelet descriptor is set at 0.5 followed by 0.3 for hue, and 0.2 for texture, then 5.25% improvement can be achieved with the proposed Dyadic wavelet descriptor, hue, and texture features.

TABLE 10 AVERAGE OF THE FEATURES AND THE PERCENT DIFFERENCE BETWEEN *CHATTNELLA ANTIQUA* AND *C.POLYKRIKOIDES*

Chttnella Antiqua		*C.Polykrikoides8cell*		% Difference
Hue	0.8133	Hue	0.9344	14.890
Texture	5.2357	Texture	4.6756	10.697
Wavelet Descriptor	0.2147	Wavelet Descriptor	0.1662	22.590
Fourier Descriptor	0.5280	Fourier Descriptor	0.4966	5.9470

TABLE 11 EUCLIDEAN DISTANCE BETWEEN *CHATTNELLA ANTIQUA* AND *C.POLYKRIKOIDES* WITH HUE, TEXTURE, AND DYADIC WAVELET DESCRIPTOR OR FOURIER DESCRIPTOR BASED SHAPE INFORMATION.

Dyadic	Fourier
0.5751	0.5739

4 Conclusion

Wavelet descriptor of shape information is effective to improve image retrieval success rate. In addition to the conventional hue and texture information, wavelet descriptor derived shape information representing contour of the object is useful for discrimination of images. Experimental results show Euclidian distance between a specific image of *Chattonella Antiqua* and the other phytoplankton with the features of hue, texture and shape information is 50 times much longer than that with the features of hue and texture information of the object image. The shortest Euclidian distance between *Chattonella Antiqua* and the other phytoplankton is improved from 0.005 to 0.24. This implies that separability between *Chatonella Antiqua* and the others is improved results in much easy image retrieval of red tide species.

It is also found that the reproducibility of the proposed Dyadic wavelet based descriptor is improved by 2-3 times in comparison to the conventional Fourier descriptor. An example for discrimination between *Chattonella Antiqua* and *C. Polykrikoides* shows 5.25% improvement can be achieved with the proposed Dyadic wavelet descriptor based features in comparison to the conventional Fourier descriptor based features if the appropriate weight factors are set to the hue, texture, and shape information of features.

Comparative study on discrimination methods for identifying dangerous red tide species based on wavelet utilized classification methods is conducted. Through experiments, it is found that classification performance with the proposed wavelet derived shape information extracted from the microscopic view of the phytoplankton is effective for identifying dangerous red tide species among the other red tide species rather than the other conventional texture, color information.

It is clear that the proposed wavelet descriptor is effective for image retrieval and classification. It is almost 40 % improvement in terms of Euclidian distance.

Normalization of features is effective to improve Euclidian distance between specie in concern and the others. The experimental results show that the Euclidian distance between *Chattnella Antiqua-3* and the others are improved remarkably, around twice much longer distance.

Acknowledgement

The author would like to thank Mr. Yuji Yamada of former student of Information Science Department of Saga University for his effort to conduct the experiments.

References

1. Duda R.O., P.E. Hart, and D.G. Stork, (2001), Pattern Classification, (Second Edition), John Wiley & Sons Inc.
2. Arai K. (1996), Fundamental theory for image processing, Gakujutsu-Tosho Shuppan Publishing Co., Ltd.
3. Séaghdha, D.O., Ann Copestake, (2009), Using lexical and relational similarity to classify semantic relations, Computational Linguistics 621-629.
4. Teh C.H. and R. T. Chin,(1988), On image analysis by the methods of moments, IEEE Trans. On Pattern Analysis and Machine Intelligence, 10, 4, 496-513

5. Taubin G. and D. B. Cooper,(1991), Recognition and Positioning of Rigid Objects Using Algebraic Moment Invariants, SPIE Conf. On Geometric Methods in Computer Vision, 1570, 175-186.
6. Niblack W.,(1993), The QBIC Project: Querying Images By Content Using Color, Texture and Shape, SPIE Conf. On Storage and Retrieval for Image and Video Databases, 1908, 173-187.
7. Zahn C.T., and Ralph Z. Roskies. (1972), Fourier Descriptors for Plane closed Curves. IEEE Trans. On Computer,c-21(3):269-281.
8. Huang C.L. and D.H. Huang,(1998), A Content-based image retrieval system. Image and Vision Computing, 16:149-163.
9. Yang H.S., S.U. Lee, K M. Lee., (1998), Recognition of 2D Object Contours Using Starting-Point-Independent Wavelet Coefficient Matching. Journal of Visual Communication and Image Representation, 9, 2, 171-181.
10. Tieng Q.M. and W. W. Boles, (1997), Recognition of 2D Object Contours Using the Wavelet Transform Zero-Crossing Representation, IEEE Trans. on PAMI 19, 8, 1997.
11. Grandlund H., (1972), Fourier preprocessing for hand print character recognition, IEEE Trans. on Computers, 621, 195-201.
12. Gibbs, J. W., (1899), "Fourier Series". Nature 59, 200 and 606.
13. Arai K. and Yasunori Terayama (2010), Polarized radiance from red tide, Proceedings of the SPIE Asia Pacific Remote Sensing, AE10-AE101-14.
14. Prasad, B E; A Gupta, H-M Toong, S.E. Madnick (1987). "A microcomputer-based image database management system". IEEE Transactions on Industrial Electronics IE-34 (1): 83–8.
15. Datta, Ritendra; Dhiraj Joshi, Jia Li, James Z. Wang (2008). "Image Retrieval: Ideas, Influences, and Trends of the New Age". ACM Computing Surveys 40 (2): 1–60
16. Duda R.O., P.E. Hart, and D.G. Stork, (2001), Pattern Classification, (Second Edition), John Wiley & Sons Inc.
17. Arai K. (1996), Fundamental theory for image processing, Gakujutsu-Tosho Shuppan Publishing Co., Ltd.
18. Séaghdha, D.O., Ann Copestake, (2009), Using lexical and relational similarity to classify semantic relations, Computational Linguistics 621-629.
19. Teh C.H. and R. T. Chin,(1988), On image analysis by the methods of moments, IEEE Trans. On Pattern Analysis and Machine Intelligence, 10, 4, 496-513
20. Taubin G. and D. B. Cooper,(1991), Recognition and Positioning of Rigid Objects Using Algebraic Moment Invariants, SPIE Conf. On Geometric Methods in Computer Vision, 1570, 175-186.
21. Niblack W.,(1993), The QBIC Project: Querying Images By Content Using Color, Texture and Shape, SPIE Conf. On Storage and Retrieval for Image and Video Databases, 1908, 173-187.
22. Zahn C.T., and Ralph Z. Roskies. (1972), Fourier Descriptors for Plane closed Curves. IEEE Trans. On Computer,c-21(3):269-281.
23. Huang C.L. and D.H. Huang,(1998), A Content-based image retrieval system. Image and Vision Computing, 16:149-163.
24. Yang H.S., S.U. Lee, K M. Lee., (1998), Recognition of 2D Object Contours Using Starting-Point-Independent Wavelet Coefficient Matching. Journal of Visual Communication and Image Representation, 9, 2, 171-181.
25. Arai K. et al. (1991), Takagi and Shimoda edt., Image Analysis Handbook, Tokyo Daigaku Shuppan-kai publishing.
26. Arai K. (1998), Methods for Image Processing and Analysis of Earth Observation Satellite Imagery Data, Morikita Shuppan Publishing Co., Ltd.
27. Arai K. and L. Jameson (2001), Earth observation satellite data analysis based on wavelet analysis, Morikita-Shuppan Publishing Co., Ltd.
28. Grandlund H., (1972), Fourier preprocessing for hand print character recognition, IEEE Trans. on Computers, 621, 195-201.
29. Gibbs, J. W., (1899), "Fourier Series". Nature 59, 200 and 606.
30. Arai K. (2002), Java based Earth observation satellite imagery data processing and analysis, Morikita-Shuppan Publishing Co., Ltd.
31. Tieng Q.M. and W. W. Boles, (1997), Recognition of 2D Object Contours Using the Wavelet Transform Zero-Crossing Representation, IEEE Trans. on PAMI 19, 8, 1997.
32. Arai K. and Yasunori Terayama (2010), Polarized radiance from red tide, Proceedings of the SPIE Asia Pacific Remote Sensing, AE10-AE101-14.

33. Arai, K., (2011), Visualization of 3D object shape complexity with wavelet descriptor and its application to image retrievals, Journal of Visualization, 15, 155-166.
34. Arai K. et al. (1991), Takagi and Shimoda edt., Image Analysis Handbook, Tokyo Daigaku Shuppan-kai publishing.
35. Arai K. (1998), Methods for Image Processing and Analysis of Earth Observation Satellite Imagery Data, Morikita Shuppan Publishing Co., Ltd.
36. Arai K. and L. Jameson (2001), Earth observation satellite data analysis based on wavelet analysis, Morikita-Shuppan Publishing Co., Ltd.
37. Arai K, (2002), Java based Earth observation satellite imagery data processing and analysis, Morikita-Shuppan Publishing Co., Ltd.